Journal of the Korean Physical Society, Vol. 32, No. , February 1998, pp. S472∼S475

Optical Properties of $RbTiOAsO_4$ Single Crystal

Chi-Shun Tu and Y. -L. Yeh

Department of Physics, Fu-Jen University, Taipei, Taiwan, Republic of China

Ram S. Katiyar and Ruqian Guo

Department of Physics, University of Puerto Rico, Rio Piedras, PR 00931, USA

V. Hugo Schmidt and Rong-Mei Chien

Department of Physics, Montana State University, Bozeman, MT 59717, USA

Ruyan Guo and A. S. Bhalla

Materials Research Lab., The Pennsylvania State University, University Park, PA 16802, USA

The longitudinal (LA) Brillouin back-scattering spectra along the [001] phonon direction have been measured over the temperature range 24-900 °C for $RbTiOAsO_4$ (RTA) single crystal. As temperature increases, the RTA shows a strong frequency softening which persists above $T_c \sim 794$ °C. The acoustic soft mode begins to set in at $T \sim 300$ °C for RTA. A broad growth was observed of both damping and susceptibility and is attributed to the dynamic order parameter fluctuations associated with a quadratic $\eta^2\mu$-type coupling (squared in order parameter and linear in strain). The refractive indices (n_x, n_y, n_z) and the Cauchy equations were obtained as a function of wavelength (0.4-1.7 μm). In addition, the LA sound velocity $V_{\rm LA}$ and elastic constant $C_{33} + (e_{33}^2/\epsilon_{33}^s)$ were also calculated at room temperature.

I. INTRODUCTION

Rubidium titanyl arsenate ($RbTiOAsO_4$) belongs to the family of nonlinear optical crystals with the general formula $M^{1+}TiOX^{5+}O_4$, where M = K, Rb, Tl, Cs and X = P, As. [1–6] The high damage threshold and broad angular acceptance have made such crystals attractive materials for frequency doubling of Nd-based lasers at λ=1.064 and 1.32 μm, and for optical parametric oscillators (OPO). In addition, the ion exchange properties also make them one of the best candidates for waveguide applications. Potassium titanyl phosphate, $KTiOPO_4$ (KTP), is the most popular among such materials and has been used successfully in different applications. However, the orthophosphate absorption at ∼4.3 and ∼3.5 μm in KTP severely limits the oscillator output power. In contrast, RTA has a broad infrared transparency (∼0.35-5.3 μm) and exhibits no overtone absorption between 3 and 5 μm. [4] This makes the RTA crystal a potential candidate for nonlinear optical applications.

At room temperature, KTP-type crystals have an orthorhombic structure with non- centrosymmetric point group C_{2v} (mm2) and space group Pna2 (Z=8). The crystal framework is a three-dimensional structure made from corner-linked TiO_6 octahedra and PO_4 tetrahedra. Four oxygen ions of the TiO_6 belong to PO_4 tetrahedral groups which link the TiO_6 groups. In our earlier Raman results, a slight softening was exhibited by several LO and TO vibrational modes of RTA. [1,2] However, there is no typical soft mode observed in the low-frequency modes of the Raman spectra. This motivated us to carry out Brillouin scattering measurements to look for softening in the acoustic modes.

We report here both the temperature-dependent acoustic phonon spectra and wavelength- dependent refractive indices. The Cauchy equations [$n(\lambda) = A + B/\lambda^2 + C/\lambda^4$] of n_x, n_y and n_z are obtained. In particular, the first direct evidence for acoustic phonon soft mode is presented.

II. EXPERIMENTAL PROCEDURE

Single crystal $RbTiOAsO_4$ was grown using the tungstate flux method. [1] The crystal was oriented by x-ray diffraction and was cut into rectangular shape having (100), (010) and (001) faces. The crystal dimension is 5.0×2.6×1.7 mm^3. The Brillouin spectra were obtained from the back-scattering geometry with config-

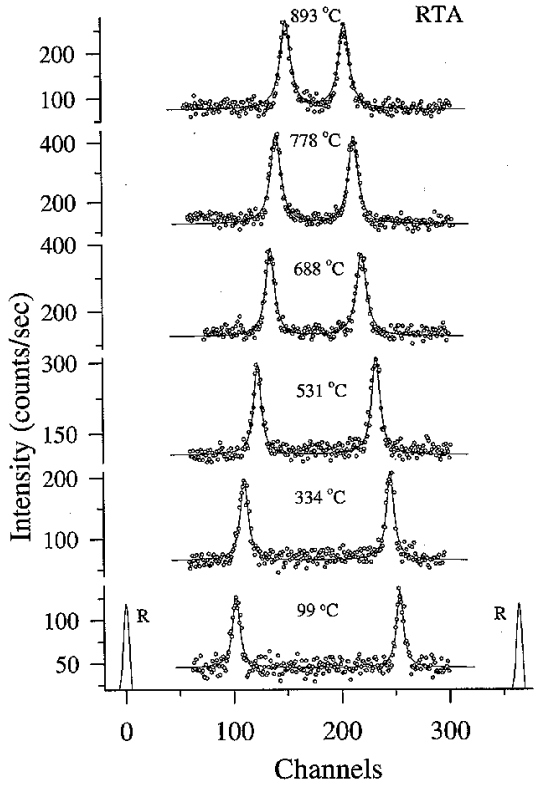

Fig. 1. Anti-Stokes and Stokes components of the LA[001] Brillouin spectra for RTA. The frequency interval (FSR) between the two Rayleigh (R) peaks is 25.79 GHz. The solid lines are fits of Eq. (1). Here, the rate of GHz/channel is 0.071.

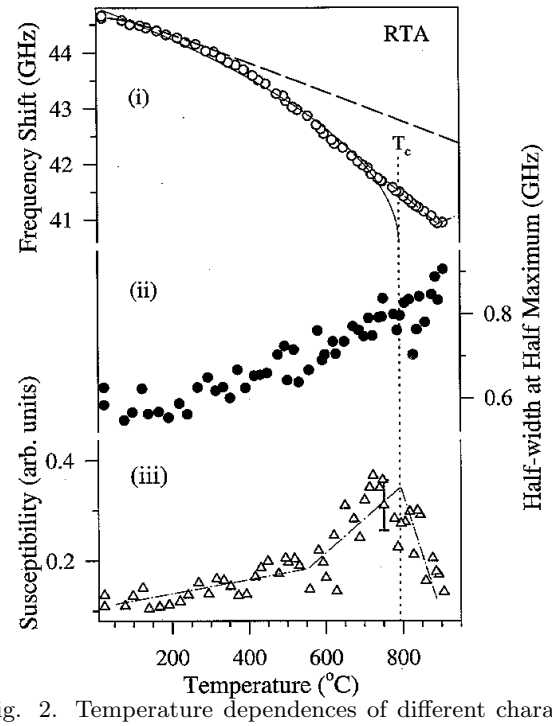

Fig. 2. Temperature dependences of different characteristics: (i) Brillouin shift (open circle), (ii) half-width (solid circle) and (iii) susceptibility constant (triangle). The dashed line is the Debye anharmonic calculation with parameters mentioned in the text. The solid line is a fit of the equation, $\omega = a(T_c - T)^{1/2} + b$. The dotted line indicates the ferroelectric phase transitions at $T_c \sim 794$ °C. The dot-dashed lines are guides to the eye.

uration $z(xu)\bar{z}$. "u" means that the collection was not polarization discriminated. Here, x and z correspond to the crystal a- and c-axes, respectively. The sample was illuminated along [001] with a Lexel Model 95-2 argon laser with λ=514.5 nm. Scattered light was analyzed by a Burleigh five-pass Fabry-Perot interferometer. To determine the positions and half-widths of the Brillouin components, the damped harmonic oscillator model with the spectral response function, [7]

$$S(\omega) = \frac{\chi_0 \Gamma \omega \omega_0^2}{(\omega^2 - \omega_0^2)^2 + \Gamma^2 \omega^2} \cdot \frac{1}{1 - e^{-\hbar\omega/kT}}, \qquad (1)$$

was used, where ω_0 and Γ correspond to the frequency and half-width, respectively, χ_0 is the susceptibility constant (in arbitrary units), k is Boltzmann's constant and T is absolute temperature.

For measurements of refractive indices, a J. A. Woollam Co. Model VB-200 Variable Angle Spectroscopy Ellipsometer was used with WVASE32^{TM} analyzing software. The refractive indices were determined by measuring the change of polarization between incident and reflected beams.

III. RESULTS AND DISCUSSION

Actual temperature-dependent LA[001] phonon spectra of both anti-Stokes and Stokes Brillouin components are shown in Fig. 1. The solid lines are fits of Eq. (1), from which the frequency shift, half-width Γ and susceptibility constant χ_0 were obtained. Fig. 2 shows the temperature dependences of the frequency shift, half-width and susceptibility constant.

In order to estimate the effect of coupling, we calculated the bare (uncoupled) phonon frequency $\omega_a(T)$ by fitting the low-temperature measured values. The bare phonon frequency is defined as the phonon frequency far from the phase transition. The temperature-dependent $\omega_a(T)$ can be described by the Debye anharmonic approximation: [8]

$$\omega_a(T) = \omega_a(0)\left[1 - A\Theta F\left(\frac{\Theta}{T}\right)\right], \qquad (2)$$

where Θ is the Debye temperature, "A" represents the amount of anharmonicity and "F" is the Debye function for internal energy, [9]

$$F\left(\frac{\Theta}{T}\right) = \frac{3}{(\Theta/T)^4}\int_0^{\Theta/T} \frac{u^3}{e^u - 1}\, du \qquad (3)$$

as tabulated, for example, by Abramowitz and Stegun. [10]

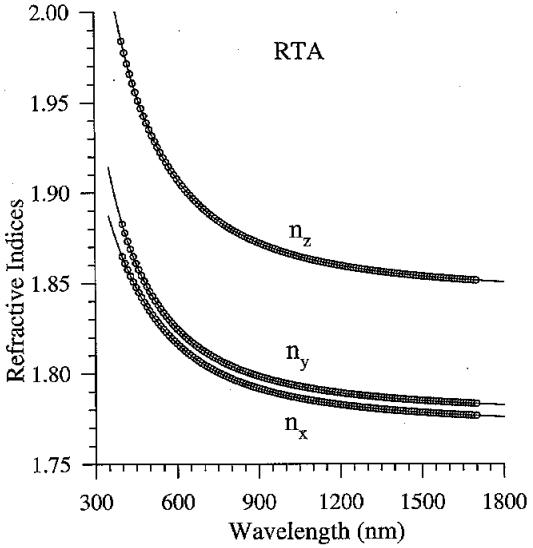

Fig. 3. Refractive indices (n_x, n_y, n_z) of RTA. Solid lines are fits to the Cauchy equations with parameters given in Eq. (4).

Table 1. Refractive indices and birefringences ($n_z - n_x$) of RTA for two wavelengths.

λ (μm)	n_x	n_y	n_z	$n_z - n_x$
0.66	1.8089	1.8165	1.8967	0.0878
1.32	1.7806	1.7872	1.8568	0.0762

In Fig. 2, the dashed line in the frequency shift is the calculation of Eq. (2) with parameters; $\omega_a(0)$=44.63 GHz, Θ=300 K and A=6×10^{-5} K^{-1}. The measured phonon frequency begins to deviate from the bare frequency at $T \sim$300 °C which corresponds to the onset of the acoustic soft mode. In addition, the solid line is fit using the equation $\omega = a(T_c - T)^{1/2} + b$, with parameters; a=0.153 (GHz/°$C^{1/2}$), b=40.53 GHz and T_c = 794 °C. We note that a zone-center (q_o=0) acoustic soft mode in the reduced Brillouin zone of the reciprocal sublattice always has a zero frequency as $T \rightarrow T_c$, *i.e.* $b = 0$. [11] However, the acoustic phonon extends its softening (with an almost constant slope) into the paraelectric phase region ($T > T_c \sim$ 794 °C). This behavior has two possible explanations: (1) the acoustic soft mode is coupled to some other excitations (perhaps the central mode) as temperature approaches the point of structural instability near T_c; (2) for such a high T_c, the lattice thermal expansion overcomes the acoustic soft mode and becomes the dominant softening effect as temperature increases.

With increasing temperature, the phonon damping (shown in Fig. 2) of RTA exhibits a gradual growth which even persists for $T > T_c \sim$ 794 °C. A similar phenomenon was also seen in the susceptibility with a broad maximum near T_c. The static Curie-Weiss form, $\chi_0 = \beta/|T_c - T|$, [11] surely cannot explain this broad anomaly. Such a slowly rising anomaly is usually associated with the dynamic order parameter fluctuations that are the characteristic mechanism of an $\eta^2\mu$-type electrostrictive coupling for longitudinal acoustic phonons. [12]

Figure 3 shows the wavelength-dependent refractive indices (n_x, n_y and n_z) of RTA measured at room temperature. The solid lines are the fits of Cauchy equations with parameters listed below:

$$\begin{aligned} n_z(\lambda) &= 1.8432 + \tfrac{0.02379}{\lambda^2} - \tfrac{0.0002041}{\lambda^4} \\ n_y(\lambda) &= 1.7773 + \tfrac{0.01722}{\lambda^2} - \tfrac{0.0000567}{\lambda^4} \\ n_x(\lambda) &= 1.7706 + \tfrac{0.01765}{\lambda^2} - \tfrac{0.0004138}{\lambda^4}. \end{aligned} \quad (4)$$

The unit of wavelength (λ) in Eq. (4) is μm. We summarize the refractive indices of two wavelengths (which could be used for frequency doubling of Nd-based lasers at λ=1.32 μm) in Table 1. The intrinsic optical birefringence of RTA decreases with increasing wavelength. The birefringence ($n_z - n_x = 0.0782$ at 1.064 μm) of RTA is smaller than for KTP ($n_z - n_x = 0.0921$ at 1.064 μm). [13] This reduction of birefringence makes RTA an ideal material for frequency doubling at higher fundamental wavelengths such as 1.32 μm for the Nd:YAG laser line.

Brillouin scattering is a powerful tool to determine the related acoustic parameters such as elastic constants. The associated theories and calculations of connected parameters can be found in Ref. [14]. At room temperature, the sample density is $\sim 4.02\times10^3$ kg/m^3 for RTA. In our experiments, the measured phonon is along the [001] direction ($\vec{q}$//[001]). By solving the secular equation (3) of Ref. [14], one obtains

$$\rho V_{LA}^2 = \rho \left(\frac{\lambda_0 \Delta\nu_{LA}}{2n \sin(\theta/2)} \right)^2 = C_{33} + \frac{e_{33}^2}{\epsilon_{33}^s} \quad (5)$$

where λ_0 is the wavelength of the incident light in vacuum, θ is the scattering angle in the crystal, $\Delta\nu_{LA}$ is the longitudinal phonon frequency shift, e_{ij} is the piezoelectric stress constant, and ϵ_{ij}^s is the static permittivity at constant strain. The related calculated values for RTA are listed followed; V_{LA}=5947 m/sec and $C_{33} + e_{33}^2/\epsilon_{33}^s = 1.42\times10^{11}$ N/m^2.

IV. CONCLUSIONS

From the temperature-dependent Brillouin spectra of RTA, two significant features have been revealed: (i) as temperature increases, the acoustic phonon soft mode becomes visible at $T \sim$ 300 °C. Specially, the acoustic softening of RTA persists above $T_c \sim$ 794 °C, which was attributed to the coupling with some other excitations (perhaps the central mode) and the lattice thermal expansion; (ii) from the temperature dependences of damping and susceptibility, we conclude that the order parameter fluctuations (associated with a quadratic $\eta^2\mu$-type electrostrictive coupling) are the dominant dynamic mechanism for the slowly rising anomalies. In addition,

the refractive indices (n_x, n_y, n_z) and the Cauchy equations of RTA were obtained as a function of wavelength (0.4-1.7 μm).

This work was supported by NSC86-2112-M-030-002 (R.O.C.), NSF Grant DMR-9520251 and DOE Grant DE-FG02-94ER75764.

REFERENCES

[1] C. -S. Tu, R. Guo, R. Tao, R. S. Katiyar, R. Guo and A. S. Bhalla, J. Appl. Phys. **79**, 3235 (1996).

[2] A. R. Guo, C. -S. Tu, R. Tao, R. S. Katiyar, Ruyan Guo and A.S. Bhalla, Ferroelectrics **188**, 143 (1996).

[3] L. K. Cheng, L. -T. Cheng, J. D. Bierlein and F. C. Zumsteg, Appl. Phys. Lett. **62**, 346 (1993).

[4] L. T. Cheng, L. K. Cheng, J. D. Bierlein and F. C. Zumsteg, Appl. Phys. Lett. **63**, 2618 (1993).

[5] G. Marnier, B. Boulanger and B. Menaert, J. Phys.: Cond. Matter **1**, 5509 (1989).

[6] L. K. Cheng, L. T. Cheng and J. D. Bierlein, Appl. Phys. Lett. **64**, 1321 (1994).

[7] J. F. Ryan, R. S. Katiyar and W. Taylor, Effet Raman et Théorie C **2**, 49 (1971).

[8] C. -S. Tu and V. H. Schmidt, Phys. Rev. B **50**, 16167 (1994).

[9] C. Kittel, *Introduction to Solid State Physics* 5th Ed. (Wiley, New York, 1976), p. 137.

[10] *Handbook of Mathematical Functions,* 7th printing, edited by M. Abramowitz and I. A. Stegun (Dover, New York, 1970), p. 998.

[11] M. E. Lines and A. M. Glass, *Principles and Applications of Ferroelectrics and Related Materials* (Oxford, London, 1977).

[12] W. Rehwald, Adv. Phys. **22**, 721 (1973).

[13] Y. F. Tso, C. E. Huang, B. Q. Hu, R. C. Eckardt, Y. X. Fan, R. L. Byer and R.S. Feigelson, Appl. Optics **26**, 2390 (1987).

[14] C. -S. Tu, V. H. Schmidt and I. G. Siny, J. Appl. Phys. **78**, 5665 (1995).